

## 3D MODE ANALYSIS OF FULL TANKS IN DRIFT-TUBE LINACS

Sergey S. Kurennoy, LANL, Los Alamos, NM 87545, USA

### Abstract

Drift-tube linacs (DTLs) are usually designed and analyzed in axisymmetric approximation, cell by cell, using 2D codes such as Superfish and Parmila. We have developed 3D models of full DTL tanks with CST Studio to accurately calculate the tank modes, their sensitivity to post-coupler positions and tilts, tuner effects, and RF-coupler influence. Such models are important for the LANSCE DTL where each of four tanks contains tens of drift tubes and tank 2 has as much as 66 cells. We perform electromagnetic analysis of the DTL tank models using MicroWave Studio (MWS), mainly with eigensolvers but also in time domain. A similar approach has already been applied for thermal analysis of the LANSCE DTL but only with short tank models [1]. The full-tank analysis allows tuning the field profile of the operating mode and adjusting the frequencies of the neighboring modes within a realistic CST model. The MWS-calculated RF fields can be used for beam dynamics and thermal modeling. Here we present beam dynamics results for the LANSCE DTL from Particle Studio.

### INTRODUCTION

The drift-tube linac (DTL) structure, proposed by Alvarez in 1946, became the most popular type of proton linacs for many decades. The DTL structure employs long cylindrical resonators (tanks) operating in  $TM_{010}$  mode and containing a sequence of drift tubes (DTs) installed along the beam axis. The DTL accelerators achieve their best efficiency for particle velocities approximately from 10% to 35% of the speed of light, i.e.  $\beta = v/c = 0.1-0.35$ . At the Los Alamos Neutron Science Center (LANSCE), the 201.25-MHz DTL covers a wider velocity range, from  $\beta = 0.04$  to 0.43 (proton energies 750 keV to 100 MeV), with the efficiency decreasing at both ends. The LANSCE DTL consists of four DTL tanks; some parameters are listed in Table 1, where  $N_{DT}$  is the number of full DTs and  $N_{pc}$  is the number of post-couplers in the tank.

Table 1: LANSCE DTL Design Parameters [2]

Parameter	Tank1	Tank2	Tank3	Tank4
Energy in, MeV	0.75	5.39	41.33	72.72
$\beta$ , in-out	0.04	0.107	0.287	.37-.43
Length $L$ , m	3.26	19.688	18.75	17.92
$N_{DT}$	30	65	37	29
$N_{pc}$	0	65	37	29
Aperture $r_b$ , cm	0.75	1-1.5	1.5	1.5
Grad. $E_0$ , MV/m	1.6-2.3	2.4	2.4	2.5
Aver. $ZT^2$ , $M\Omega/m$	26.8	30.1	23.7	19.2

### DTL TANK MODELS

We have built 3D models of the four DTL tanks in the CST Studio [3] using CST geometrical macros and tank element dimensions from the LANSCE database. The CST model of tank 2 (T2) is illustrated in Fig. 1. This is the longest DTL tank that contains 65 full DTs and two half-DTs on the end walls. The full DTs are supported by vertical stems. The tank cavity of radius 45 cm is shown in Fig. 1 as the blue-gray cylinder, which is assumed to be surrounded by perfect conducting walls for field calculations. Two upper insets show side views near the tank entrance (blue) and its exit (green). The stabilizing post-couplers (gray) with rotating tabs alternate positions in the horizontal plane; they can be seen better in the end view of the tank in the right-bottom inset.

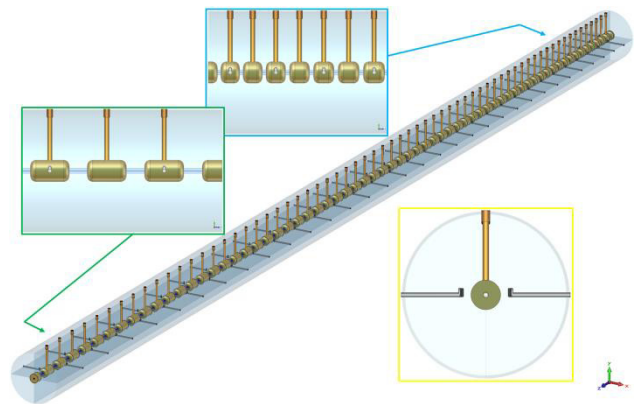


Figure 1: CST model of the DTL tank 2.

The CST model of tank 4 (T4) with 8 frequency slug tuners (cyan) is shown in Fig. 2. The left inset enlarges details: the bellows near the stem connection to the cavity wall are modeled as metal cylinders; the blue line through DT apertures indicates the beam axis.

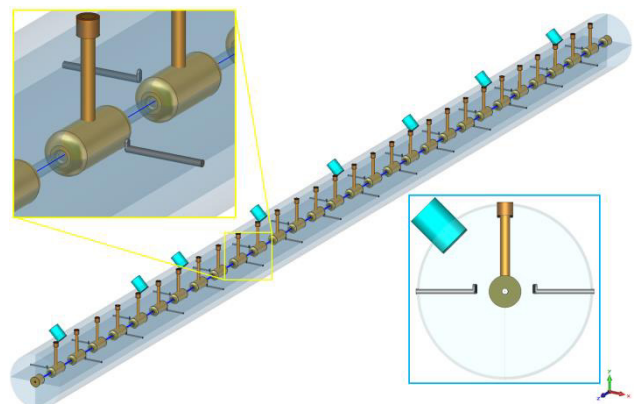


Figure 2: CST model of tank 4 with frequency tuners.

Unlike long tanks 2 to 4, the relatively short tank 1 (T1) does not have post-couplers. One the other hand, the

accelerating field in T1 is ramped: it increases along the tank, with the minimum average cell field  $E_{0, \min} = 1.6$  MV/m and maximum  $E_{0, \max} = 2.3$  MV/m. In T2 to T4, the accelerating gradient (average cell field)  $E_0$  is constant. It is tuned to be flat by adjusting spacing between post-couplers and DTs and, more finely, by rotating tabs. In T1, the ramp is adjusted by two tilt tuners that deform the tank end walls: the upstream wall is pushed in and the downstream one out.

### RF FIELDS IN DTL TANKS

The fields in the tank models were calculated using CST MicroWave Studio (MWS). The most efficient was its tetrahedral eigensolver; we also used the hexahedral eigensolver AKS and time-domain analysis. For accurate computations the meshes were refined locally, especially inside an artificial vacuum cylindrical insert covering the DT apertures; see the narrow dark-gray cylinder around the beam axis in the left inset of Fig. 2. More details of MWS computations can be found in [4].

When the tank models T2-4 have the measured post-coupler spacing distances and tab rotation angles, the calculated field profiles of the operating mode along the tank are not flat [4]. Likely, the distances were adjusted following field measurements to compensate real-tank imperfections. We tune these parameters in the CST models to flatten the field of the operating mode and adjust its frequency separations from two neighboring modes. As an example, the tuned on-axis accelerating field in T2 is plotted in Fig. 3. Note that the peaks in the gaps become two-pronged near the tank end where the gaps are wider, cf. Fig. 1. This effect is more pronounced in T3 and T4, which have much wider gaps between DTs.

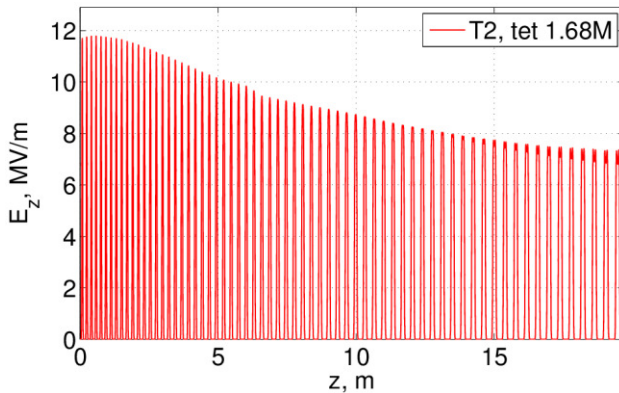


Figure 3: On-axis longitudinal electric field in tank 2.

The corresponding average cell fields (gradients) in T2 are plotted in Fig. 4: they are within  $\pm 1.5\%$  of the design gradient  $E_0 = 2.4$  MV/m. Similarly, in the T1 model we tune the field gradient ramp by adjusting the penetration depths of two tilt tuners on the tank end walls.

Interesting to note that tuning the profile flatness for the operating mode in T2-4 also provides almost equal separations of the operating mode frequency from the two neighboring modes. The frequency spectrum of the tank modes is easier to calculate with the AKS eigensolver.

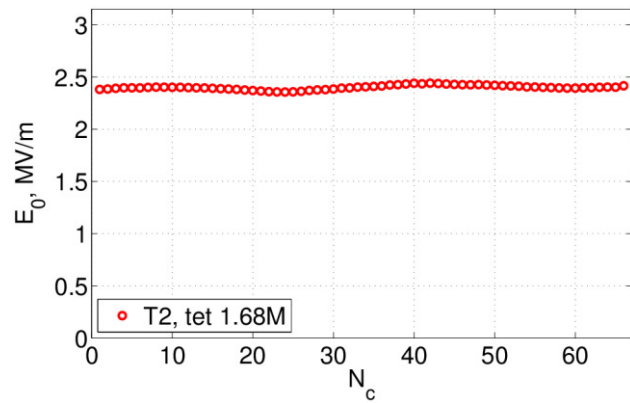


Figure 4: Average accelerating field in 66 cells of tank 2.

One should note that the operating mode number is rather high in tanks with many DTs,  $N_o = N_{DT} + N_{pc} + 1$ . From Table 1,  $N_o = 59$  in T4 and is as high as 131 in T2! We need to calculate more than  $N_o$  modes with the AKS eigensolver, which is difficult but doable. The mode frequency spectra in tanks 1 and 4 were discussed in [4].

The MWS results were used to calculate various tank parameters. The total dissipated power for the operating mode and its distribution between the tank elements are in an excellent agreement with the results [1] derived from a piece-wise analysis of individual cells with MWS. Only about 3-4% of the RF losses are deposited on post-couplers. However, for other modes the surface-loss distribution is significantly different: in post-coupler modes more than 60% is deposited on the post-couplers, and in higher modes, this amount is at least 40%.

### BEAM DYNAMICS

The MWS-calculated RF fields of the tuned operating mode in the DTL tanks are now available to study beam dynamics in the LANSCE DTL. It can be done with various multi-particle codes; we use CST Particle Studio (PS). The static magnetic fields of focusing quadrupoles, produced in Matlab as text files based on tables of the quad design values, are imported into PS as external fields. Two initial particle distributions at the T1 entrance were provided by L. Rybarcyk. The first one started as a distribution of 10K macro-particles corresponding to the 24-mA current that was run through the future LANL RFQ [5] and the following beam transfer; 9587 particles (23 mA) reach the T1 entrance. The other distribution from the existing Cockcroft-Walton (C-W) injector was traced through the existing transport lines that include a pre-buncher; 10K macro-particles at the entrance of tank 1 correspond to the 18-mA current into T1. The beam parameters at the T1 entrance are as follows: the average beam energy  $W = 0.75$  MeV; for the 23-mA case, the normalized rms horizontal emittance  $\epsilon_x = 0.29 \pi \mu\text{m}$  and vertical one  $\epsilon_y = 0.28 \pi \mu\text{m}$ ; for the CW 18-mA case, the emittances are  $\epsilon_x = 0.12 \pi \mu\text{m}$  and  $\epsilon_y = 0.10 \pi \mu\text{m}$ .

The PS particle-in-cell (PIC) solver runs the input distribution through a tank with RF and quadrupole fields and records the particles in the exit plane. The exit

distribution serves as an input for the next simulation stage, which is a drift space between two tanks, and so on. To ensure the correct RF phases,  $-26^\circ$  in all tanks, the input distributions are time-delayed for the bunch center to reach the middle of the first RF gap exactly at  $-26^\circ$ . To reduce the mesh size for PS runs, we cut the tank volume in the transverse directions  $x$  and  $y$  just outside the DTs, but at the same time refine the mesh within DT apertures. Comparing PS results from such cut models and full-volume ones for a few test cases showed no differences. As an illustration of PS output, a snapshot of the 23-mA bunch near the exit of T4, in its last half-DT, is shown in Fig. 5. There are 9016 particles in the bunch. The particle energies are close to 100 MeV as indicated by color; see the energy scale on the right. The particle energies at the T4 entrance were around 72.5 MeV.

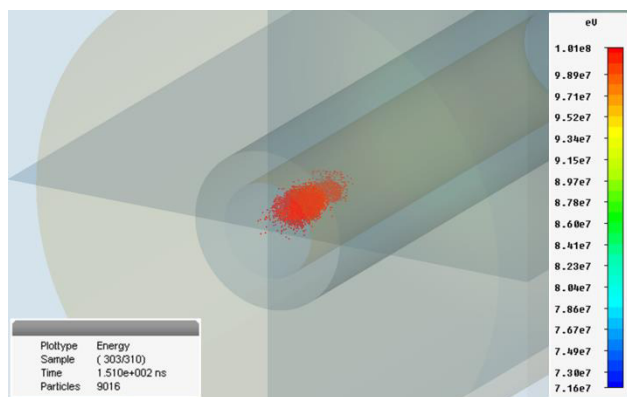


Figure 5: Particles near tank 4 exit in PS run with 23 mA.

Our PS simulation results for the two initial beam distributions are summarized in Tables 2-3.

Table 2: PS Simulation Results for 23-mA Case

Parameter	T1 out	T2 out	T3 out	T4 out
Aver. $W$ , MeV	5.37	41.36	72.53	100.16
Transmission	0.94*	1	1	1
$\epsilon_x$ , $\pi \mu\text{m}$	0.35	0.43	0.44	0.44
$\epsilon_y$ , $\pi \mu\text{m}$	0.37	0.33	0.37	0.38
$\epsilon_z$ , $\pi \mu\text{m}$	2.26	1.96	2.08	2.16

Table 3: PS Simulation Results for C-W 18-mA Case

Parameter	T1 out	T2 out	T3 out	T4 out
Aver. $W$ , MeV	5.36	41.36	72.53	100.16
Transmission	0.81*	1	1	1
$\epsilon_x$ , $\pi \mu\text{m}$	0.30	0.35	0.36	0.36
$\epsilon_y$ , $\pi \mu\text{m}$	0.24	0.24	0.27	0.30
$\epsilon_z$ , $\pi \mu\text{m}$	1.96	1.69	1.87	2.12

The beam transmission values (\*) after T1 include only particles exiting in a well-formed bunch. There are other particles that exit T1 with lower energies. They will be

lost eventually, mainly in T2, so we do not take them into account to speed up PS runs for T2-4.

Most beam parameters do not depend on the mesh size for PS runs with meshes from a few million to 56M mesh points. The transverse emittances initially increase as the mesh size increases but then stay practically constant. Most of the above PS results were obtained with meshes  $\sim 35\text{M}$  points. Such PS runs take overnight on a PC.

## CONCLUSION

We built and studied realistic 3D models of all four tanks in the LANSCE DTL. Electromagnetic analysis of the models was performed using MWS. The tank RF fields were calculated and relevant cavity parameters were derived. We explored how the fields of the operating mode depend on settings of post-couplers and frequency tuners in T2-4 and on tilt tuners in T1. Of particular interest was tuning the flatness of the field profile along the tanks 2-4 and the frequency separations of the operating mode from its neighbors by adjusting spacing distances between DTs and post-couplers. Many results agree well with previous calculations that used either separate cells or short sections of the tank; for example, surface-loss power and its distribution between the tank elements. One unexpected result was that tab rotations can produce not only localized changes of the field profile but also global ones, distributed over the whole tank [4].

Two realistic beam distributions were propagated through the DTL with the Particle Studio PIC solver using the MWS-calculated RF fields. These fields can also be exported and used in other multi-particle codes. Our PS results agree with expectations.

Overall, studying realistic models of all DTL tanks is important for better understanding of the LANSCE DTL. Future developments may include exploring RF power couplers attached to the full tank models, more detailed study of field tuning, and possibly multipacting effects in the DTL tanks with RF couplers.

## ACKNOWLEDGMENT

The author would like to thank J. O'Hara, L. Rybarcyk, R. Garnett, and Y. Batygin (LANL) for useful information and stimulating discussions.

## REFERENCES

- [1] S.S. Kurennoy, "Surface-Loss Power Calculations for the LANSCE DTL," Linac'08, Victoria, BC, Canada, p. 951 (2008); www.JACoW.org
- [2] T.P. Wangler, *RF Linear Accelerators*, (Wiley-VCH, 2<sup>nd</sup> Ed., 2008), p. 95.
- [3] CST Studio Suite, CST, www.cst.com
- [4] S.S. Kurennoy, "RF Fields in LANSCE DTL Tanks," LANL report AOT-HPE 14-005, Los Alamos, 2014.
- [5] R.W. Garnett et al, "Status of the LANSCE Front End Upgrade," PAC2013, Pasadena, CA, USA, p. 327 (2013); www.JACoW.org